

PAPER • OPEN ACCESS

Electrochromism in sputter deposited $W_{1-y}Mo_yO_3$ thin films

To cite this article: M A Arvizu *et al* 2016 *J. Phys.: Conf. Ser.* **682** 012005

View the [article online](#) for updates and enhancements.

You may also like

- [Compound semiconducting SnSb alloy anodes for Li ion batteries: effect of elemental composition of Sn–Sb](#)
Lakshmi D, Jayapandi S, Nalini B et al.
- [Intense Red-Emitting NaYSiO₄: Eu₃₊, Mo₆₊ Phosphors for White Light-Emitting Diodes](#)
Yan Wen, Yuhua Wang, Feng Zhang et al.
- [Spin density wave behaviour in the \(Cr_{100-x}Al_{1-x}\)₄Mo₅ and \(Cr_{100-x}Al_{1-x}\)₃Mo₅ alloy series](#)
B Muchono, ARE Prinsloo, CJ Sheppard et al.

ECS
The
Electrochemical
Society
Advancing solid state &
electrochemical science & technology

DISCOVER
how sustainability
intersects with
electrochemistry & solid
state science research

Electrochromism in sputter deposited $W_{1-y}Mo_yO_3$ thin films

M A Arvizu, C G Granqvist and G A Niklasson

Department of Engineering Sciences, The Ångström Laboratory, Uppsala University,
P. O. Box 534, SE-751 21 Uppsala, Sweden

E-mail: Miguel.Arvizu@angstrom.uu.se

Abstract. Electrochromic (EC) properties of tungsten–molybdenum oxide ($W_{1-y}Mo_yO_3$) thin films were investigated. The films were deposited on indium tin oxide covered glass by reactive DC sputtering from tungsten and molybdenum targets. Elemental compositions of the $W_{1-y}Mo_yO_3$ films were determined by Rutherford back scattering. Voltammetric cycling was performed in an electrolyte of 1 M $LiClO_4$ in propylene carbonate. An increase in molybdenum content in the EC films caused both a shift towards higher energies and a lowering of the maximum of the optical absorption band, as compared with WO_3 EC films. Durability under electrochemical cycling was diminished for $W_{1-y}Mo_yO_3$ EC films.

1. Introduction

Electrochromic (EC) materials are capable of undergoing reversible optical changes when an electrochemical potential is applied. The applied voltage causes double insertion/extraction of electrons from a back contact and ions from an electrolyte [1]. Among the materials exhibiting electrochromism, inorganic compounds (mainly transition metal oxides) are widely studied and have been used in industrial applications as well; for example so called “smart windows” are devices that allow the user to control the transmission of solar energy and visible light [2]. Tungsten trioxide (WO_3) is the most common inorganic EC material, and a lot of research has been carried out to investigate its properties through the years [1–4]. From the first studies on electrochromism of tungsten trioxide, it is well known that in the dark state WO_3 films acquire an intense blue color due to the formation of a wide absorption band centred around 1.3 to 1.45 eV [5,6]. Electrochromic properties in molybdenum oxide (MoO_3) were discovered a few years after the phenomenon was shown to exist in WO_3 [7]. Very soon an attempt to combine both oxides and study the effects of mixing them was carried out. Hence EC thin films were produced by co-evaporation from WO_3 and MoO_3 powders, and the outcome of those experiments was the discovery of a shift towards higher energy of the maximum of the absorption band of the mixed oxide films as compared to pure WO_3 [8]. Further studies on co-evaporated W–Mo oxides showed the existence of two types of absorption bands for molybdenum oxide; one is equivalent to the band formed in the colored state of WO_3 , the so called G-band centred between 1.5 and 1.56 eV; this is the only band present in the case of small charge insertion. By increasing the amount of inserted charge an additional band, called the T-band, appears between the G-band and the interband absorption across the band gap. The T-band becomes predominant and the G-band decreases for high values of inserted charge [9]. Other synthesis techniques have also been used in order to get tungsten–molybdenum oxide EC films. Electrochemical deposition from a metal peroxide leads to enhanced dynamical optical response for small contents of molybdenum (<2%) which respect to pure WO_3 films [10]. $W_{1-y}Mo_yO_3$ thin films prepared by atmospheric pressure chemical vapor deposition showed improved EC performance with higher dark-



state optical absorption, the center of the absorption closer to the peak of the eye's sensitivity and good coloration efficiency [11]. Molybdenum-doped spray pyrolysed WO_3 EC films showed a different microstructure and crystallinity, together with better EC response for nominal concentrations around 6% Mo and better electrochemical stability for small nominal concentrations (~2% Mo) as compared with pure tungsten oxide films [12]. In this present work we prepared $\text{W}_{1-y}\text{Mo}_y\text{O}_3$ EC thin films by sputtering and studied their EC performance with focus on durability issues.

2. Film deposition and composition

2.1. Sputter deposition

Thin films of W oxide, Mo oxide and W–Mo oxide were prepared by reactive DC magnetron sputtering in a deposition system based on a Balzers UTT 400 unit. Targets were 5-cm-diameter plates of W and Mo (Plasmaterials), all with 99.99% purity. The sputter system was evacuated to 2×10^{-4} mTorr. Argon and oxygen, both of 99.997% purity, were then introduced through mass-flow controlled gas inlets. Substrates for optical and electrochemical measurements were unheated 5×5 cm² glass plates coated with transparent and electrically conducting layers of $\text{In}_2\text{O}_3:\text{Sn}$ having a resistance of 40 Ω /square. The target–substrate separation was 13 cm. Film thicknesses were ~300 nm as determined by surface profilometry using a Bruker DektakXT instrument. Pure WO_3 and MoO_3 films were obtained using solely the W and Mo targets, respectively, with an O_2/Ar ratio set to 0.14 and a working pressure of ~30 mTorr. The discharge power P was set to 225 W for the tungsten oxide samples and 300 W for molybdenum oxide. For the $\text{W}_{1-y}\text{Mo}_y\text{O}_3$ films, co-sputtering from W and Mo targets was performed with an O_2/Ar ratio set to 0.28 and using the same working pressure of ~30 mTorr. To change the composition of the resulting films, P was kept constant for the W target at 225 W while varying the Mo discharge power between 125 and 300 W. Films for Rutherford backscattering spectrometry (RBS) were deposited onto carbon plates. All deposited films presented X-ray diffraction patterns characteristic of amorphous materials.

2.2. Compositional characterization

Elemental characterization of the films was performed with RBS using 2 MeV ^4He ions backscattered at an angle of 170°. With these conditions it is possible to get up to 2 μm analysis depth with high sensitivity for heavy elements such as Mo and W. The RBS data were fitted to a model of the film–substrate system by use of the SIMNRA simulation program [13]. The resulting composition of the $\text{W}_{1-y}\text{Mo}_y\text{O}_3$ films is shown in table 1.

Table 1. Composition of $\text{W}_{1-y}\text{Mo}_y\text{O}_3$ films.

Plasma power of Mo target [W]	Mo content ($y \pm 0.01$)
125	0.02
150	0.04
175	0.08
200	0.10
225	0.14
250	0.16
275	0.22
300	0.30

3. Electrochemical data

Cyclic voltammetry (CV) measurements were performed using a Solartron 1286 Electrochemical Interface in a three-electrode electrochemical cell. The electrolyte was 1 M LiClO_4 in propylene

carbonate, and lithium foils served as reference and counter electrodes. All measurements were performed inside a glove box with inert argon atmosphere. The voltage sweep rate was 10 mV/s.

WO_3 and $\text{W}_{1-y}\text{Mo}_y\text{O}_3$ are electrochemically stable when cycled hundreds of times in the voltage range 2.0–4.0 V vs. Li, and for WO_3 this is in accordance with previous findings [14]. MoO_3 is also stable, but in the range 2.5–4.5 V vs. Li. In order to accelerate the ageing process of the films, it is possible to increase the voltage range to 1.7–4.0 V vs. Li [14]. This procedure accelerates degradation by about a factor ten [14]. Figure 1 shows cyclic voltammograms for chosen $\text{W}_{1-y}\text{Mo}_y\text{O}_3$ films in that range, and in all cases fast degradation occurs within 80 CV cycles. The ageing seems to happen earlier for films containing molybdenum, but the voltammograms for these films tend to stabilize at some point and this happens earlier when more Mo is present. It is also interesting to note the appearance of a shoulder in the CV data with regard to the current density at around 3.0 V vs. Li in the insertion part of the cycle for samples with Mo contents $y > 0.14$. At potentials lower than 2.5 V vs. Li, the voltammograms follow the usual behavior for WO_3 EC films. This shoulder, although less noticeable, tends to shift to lower voltage as the number of cycles is increased.

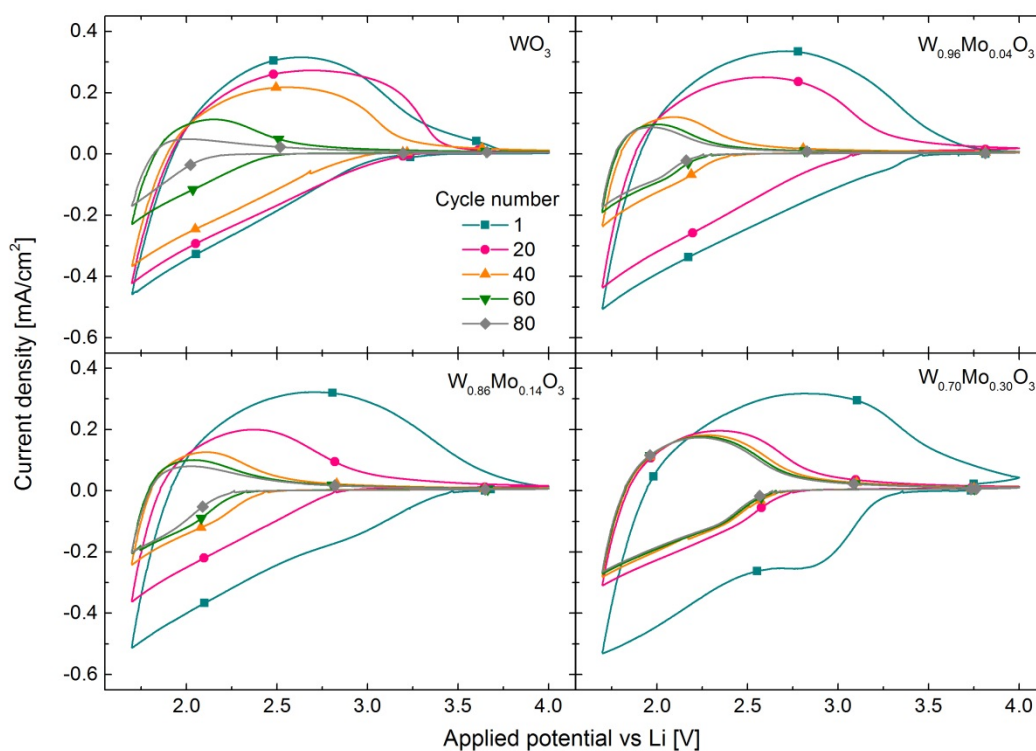


Figure 1. Cyclic voltammograms for W–Mo oxide films of the shown compositions. Data were taken after the indicated numbers of cycles and for the voltage sweep range 1.7–4.0 V vs. Li.

In order to further investigate the electrochemical reversibility, figure 2 shows the difference between inserted and extracted charge densities for successive voltammetric cycles defined [14] as $\delta Q = |Q_{\text{inserted}} + Q_{\text{extracted}}|$; the absolute value is necessary to assure that δQ is a positive quantity, since we follow the convention $Q_{\text{inserted}} < 0$, $Q_{\text{extracted}} > 0$. Here it is confirmed that for the $\text{W}_{1-y}\text{Mo}_y\text{O}_3$ EC films the inserted charge is larger than the extracted charge in the first cycles, and this tendency increases with increasing Mo content. Equilibrium between inserted and extracted charge is reached faster than for pure WO_3 films. This difference between inserted and extracted charge could be due to trapped lithium ions that tend to accumulate in the films, and as a consequence ion intercalation becomes more difficult and the films start to acquire a permanent yellowish coloration.

However, a depth-profiling elemental analysis of as-deposited and intercalated samples is necessary in order to confirm this supposition. In the next section we show how the optical modulation is affected when the $W_{1-y}Mo_yO_3$ EC films are cycled in the stated voltage range and the number of cycles is increased.

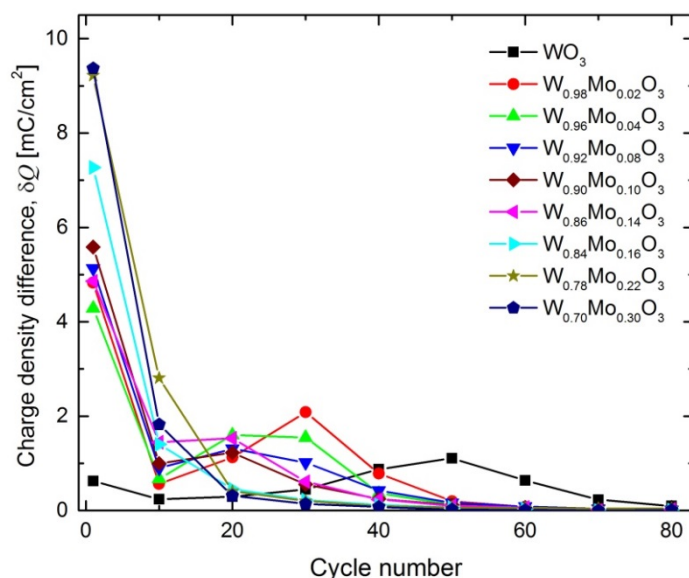


Figure 2. Evolution of the difference in charge density for charge insertion and extraction δQ , as a function of cycle number, for $W_{1-y}Mo_yO_3$ EC films. Symbols denoting data were joined by straight lines.

4. Optical measurements

4.1. *In situ* optical transmittance

When the samples were cycled in the voltage range 1.7–4.0 V vs. Li, monochromatic optical transmittance T at the mid-luminous wavelength 550 nm was registered using an Ocean Optics fiber-optic instrument. In figure 3 it is seen that the transmittance modulation $\Delta T = T_{\text{bleached}} - T_{\text{colored}}$ decreases as the number of cycles increases. It is clear that for high Mo content, $W_{1-y}Mo_yO_3$ EC films quickly lose most of their EC capacity, since the diminishing charge capacity in the films is accompanied by poor optical response. Moreover all samples eventually attained a permanent yellowish color, which is another indication of film degradation when cycling in the wide voltage window.

4.2. *Optical absorption spectra*

We now discuss the effect of Mo doping on the optical response of the tungsten oxide EC film in the colored state. The WO_3 and $W_{1-y}Mo_yO_3$ EC films were cycled in the voltage range 2.0–4.0 V vs. Li, while the MoO_3 EC film was cycled at 2.5–4.5 V vs. Li. After the 20th cycle, the CV data were stopped at the state of maximum coloration, the film was taken out from the glovebox, gently rinsed with isopropanol, dried with a nitrogen gun, and its spectral optical transmittance $T(\lambda)$ and reflectance $R(\lambda)$ were immediately measured in the $300 < \lambda < 2500$ nm interval using a Perkin–Elmer Lambda 900 spectrophotometer. The resulting data were then used to obtain the optical absorption coefficient using the approximate expression

$$\alpha = \frac{1}{d} \ln \left(\frac{1-R(\lambda)}{T(\lambda)} \right) \quad (1)$$

which is valid for weakly absorbing films on glass substrates, provided the refraction index of the glass is 1.5–1.7 [15]. Here d is film thickness. Figure 4 shows spectral absorption coefficient of the films as a function of photon energy for the WO_3 , $\text{W}_{1-y}\text{Mo}_y\text{O}_3$ and MoO_3 EC films. The spectrum for WO_3 is typical with the maximum of the absorption band around 1.45 eV. For MoO_3 , a wide absorption band around 2.19 eV is formed by the T-component and the diminished G-band. The effect of increasing Mo content in the $\text{W}_{1-y}\text{Mo}_y\text{O}_3$ films is twofold; firstly the maximum of the absorption band is shifted toward higher energies (it is clearly positioned at 1.71 eV for the $\text{W}_{0.92}\text{Mo}_{0.08}\text{O}_3$ sample) and the samples look grey instead of bluish, and secondly the maximum value diminishes and the absorption spectra became flattened. Very likely the T-component absorption in MoO_3 starts to dominate the optical behavior for the binary oxide films.

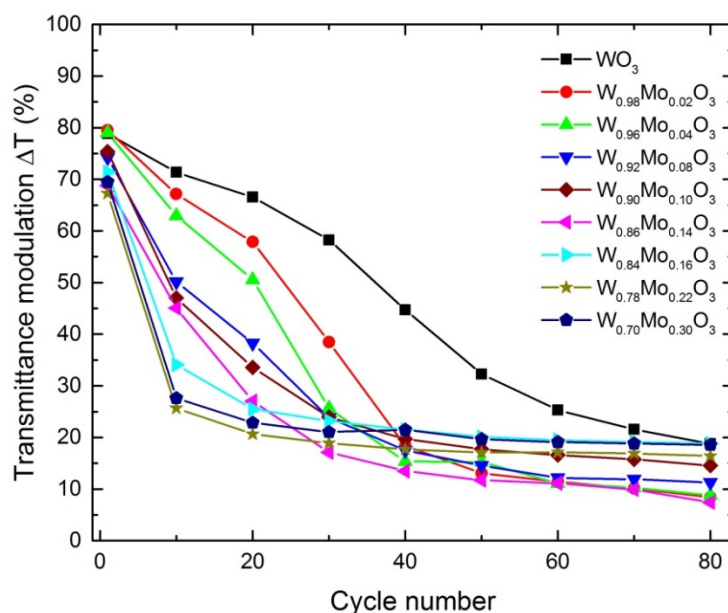


Figure 3. Evolution of the transmittance modulation ΔT at the wavelength 550 nm for films of the shown compositions. Data were taken after the indicated numbers of cycles and for the voltage sweep range 1.7–4.0 V vs. Li. Symbols denoting data were joined by straight lines.

5. Conclusions

Electrochromic DC sputtered thin films of WO_3 , MoO_3 and $\text{W}_{1-y}\text{Mo}_y\text{O}_3$ were studied and compared as regards their optical properties and degradation. When the Mo content is increased in $\text{W}_{1-y}\text{Mo}_y\text{O}_3$ films the durability of the samples, as measured by the charge capacity and the optical transmittance modulation, decreases considerably when the potential sweep range is 1.7–4.0 V vs. Li. In addition, when the potential sweep range is 2.0–4.0 V vs. Li, the optical absorption decreases and its spectral dependence is drastically flattened. The resulting films are greyish in the colored state and there is a clear tendency of the maximum of the absorption band to shift toward higher energies, as compared to pure WO_3 , at least at low Mo content. Hence, the mixed oxides can be used for “smart windows” in order to get a more neutral dark state, although at the same time somewhat compromising the durability and coloration intensity of the device.

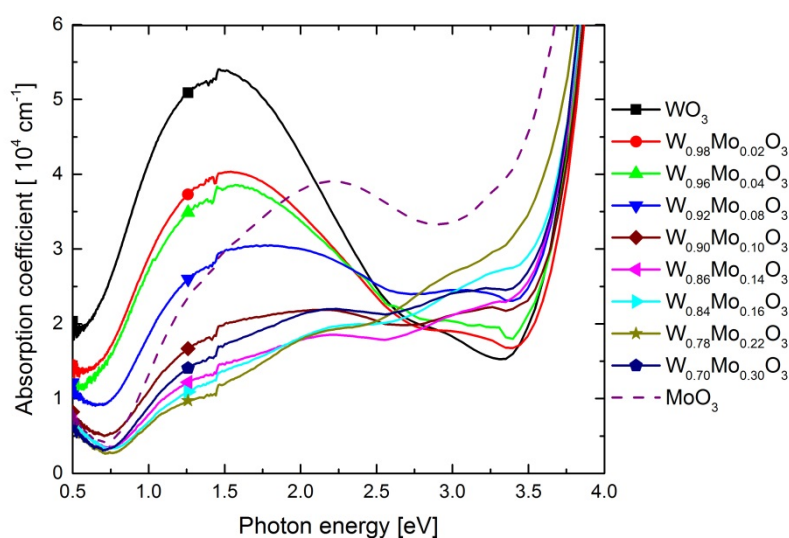


Figure 4. Optical absorption coefficient as a function of energy, in the maximum coloration (dark) state after 20 CV cycles for films of the shown compositions.

Acknowledgements

This paper was presented at the INERA Conference "Light in Nanoscience and Nanotechnology", Oct. 19-22, 2015, Hissar, Bulgaria. The conference is part of the program INERA REPGOT project of the Institute of Solid State Physics, Bulgarian Academy of Sciences. We are grateful to Daniel Primetzhofer and the staff of the Tandem Accelerator Laboratory at Uppsala University for support with RBS measurements. MAA thanks the Mexican Council for Science and Technology (CONACyT) for financial assistance to carry out postdoctoral research at Uppsala University. Our work was supported by the European Research Council under the European Community's Seventh Framework Program (FP7/2007–2013)/ERC Grant Agreement No. 267234 ("GRINDOOR").

References

- [1] Granqvist C G 1995 *Handbook of Inorganic Electrochromic Materials* (Amsterdam: Elsevier)
- [2] Granqvist C G 2014 *Thin Solid Films* **564** 1–38
- [3] Granqvist C G 2000 *Sol. Energy Mater. Sol. Cells* **60** 201–62
- [4] Wen R-T, Arvizu M A, Niklasson G A and Granqvist C G 2015 *Surf. Coat. Tech.* **278** 121–25
- [5] Deb S K 1969 *Appl. Opt. Suppl.* **3** 192–95
- [6] Deb S K 1973 *Philos. Mag.* **27** 801–22
- [7] Deb S K 1975 *Proc. 4th Int. Cong. Reprography and Information* (Hannover, Germany) 115–19
- [8] Faughnan B W and Crandall R S 1977 *Appl. Phys. Lett.* **31** 834–36
- [9] Hiruta Y, Kitao M and Yamada S 1984 *Jpn. J. Appl. Phys.* **23** 1624–27
- [10] Pennisi A, Simone F and Lampert C M 1992 *Sol. Energy Mater. Sol. Cells* **28** 233–47
- [11] Gesheva K, Szekeres A and Ivanova T 2003 *Sol. Energy Mater. Sol. Cells* **76** 563–76
- [12] O-Rueda de León J M, Acosta D R, Pal U and Castañeda L 2011 *Electrochim. Acta* **56** 2599
- [13] Mayer M 1999 *AIP Conf. Proc.* **475** 541–44
- [14] Arvizu M A, Triana C A, Stefanov B I, Granqvist C G and Niklasson G A 2014 *Sol. Energy Mater. Sol. Cells* **125** 184–89
- [15] Hong W Q 1989 *J. Phys. D: Appl. Phys.* **22** 1384–85